

# EPITAXY AND CRYSTALLOGRAPHIC TEXTURE OF THIN FILMS FOR MAGNETIC RECORDING

DAVID E. LAUGHLIN,\* Y.C. FENG, LI-LIEN LEE\* AND B. WONG

Materials Science and Engineering Department, Carnegie Mellon University

\*Data Storage Systems Center, Carnegie Mellon University, Pittsburgh, PA 15213

## ABSTRACT

Thin films for magnetic recording are usually deposited on metallic Cr underlayers to control their crystallographic texture and such microstructural features as grain size and crystal perfection. In this paper, the mechanisms involved in the production of thin films (both underlayers and magnetic layers) with specific crystallographic textures is reviewed and discussed. We first present an overview of a model for the development of the initial crystallographic texture of films grown on amorphous substrates. The textures that various structures develop during growth are next discussed followed by a review of the role of epitaxy of Co-alloy films with underlayers and interlayers. The control of grain size of the magnetic film is also discussed in light of the underlayer grain size. Finally, the role of epitaxy on the crystalline perfection and subgrains with the underlayer (Cr and/or NiAl) is introduced.

## INTRODUCTION

It is well known that the crystallographic texture of thin films for magnetic recording has a profound influence on the recording properties of the films<sup>1-6</sup>. A schematic of a cross section of thin film recording media is shown in Figure 1. In this paper we will discuss the development of the crystallographic texture of the underlayer film as well as the development of the crystallographic texture of the magnetic layer. Over the last decade or so a plethora of data has been collected and published concerning the crystallographic texture of both the underlayers and the magnetic layers.<sup>7-17</sup> In the main, the basic mechanisms for the development of crystallographic texture in the Cr underlayers seems to depend on the interplay between the energetics and growth of the films, while the basic mechanism for the development of the texture of Co alloy magnetic thin films is one of epitaxy. In this paper we will discuss both of these general mechanisms of crystallographic texture formation. In the first section a model for the understanding of the development of either the (110) or (002) texture in Cr films grown on amorphous substrates will be presented and illustrated. In the second section we will summarize the various epitaxial relations observed to date between hcp Co alloy thin films and bcc Cr underlayers. In the third section we will briefly discuss the effect of underlayers and interlayers on the grain size and crystalline perfection of the magnetic layers.

## I. DEVELOPMENT OF UNDERLAYER CRYSTALLOGRAPHIC TEXTURE

We start our discussion with the case of bcc Cr underlayers. It is well known that by changing the substrate preheating temperature two different crystallographic textures can be produced in Cr thin films. The normally obtained crystallographic texture is (110). However, under specific conditions, the (002) Cr texture can be obtained. These are the two crystallographic textures for Cr underlayers that are most frequently reported in the literature.

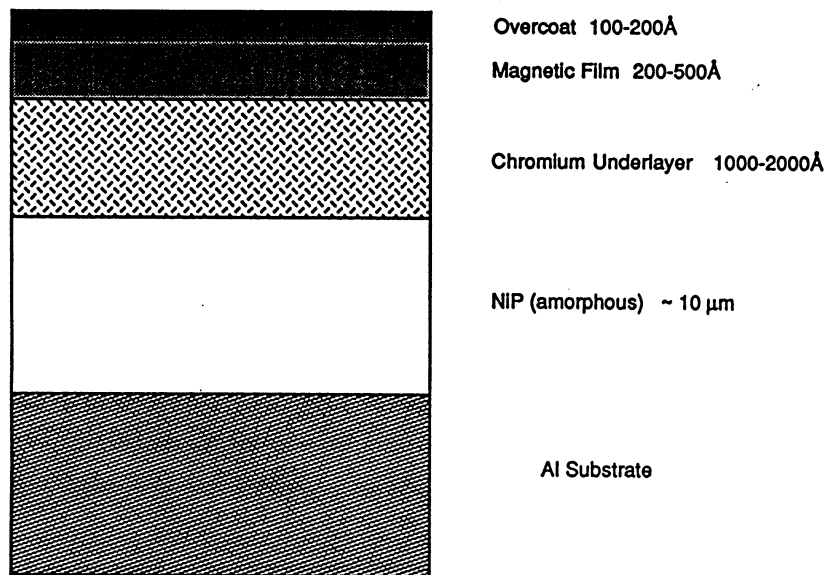


Figure 1. A schematic of the cross section of a typical hard disk media. Not to scale.

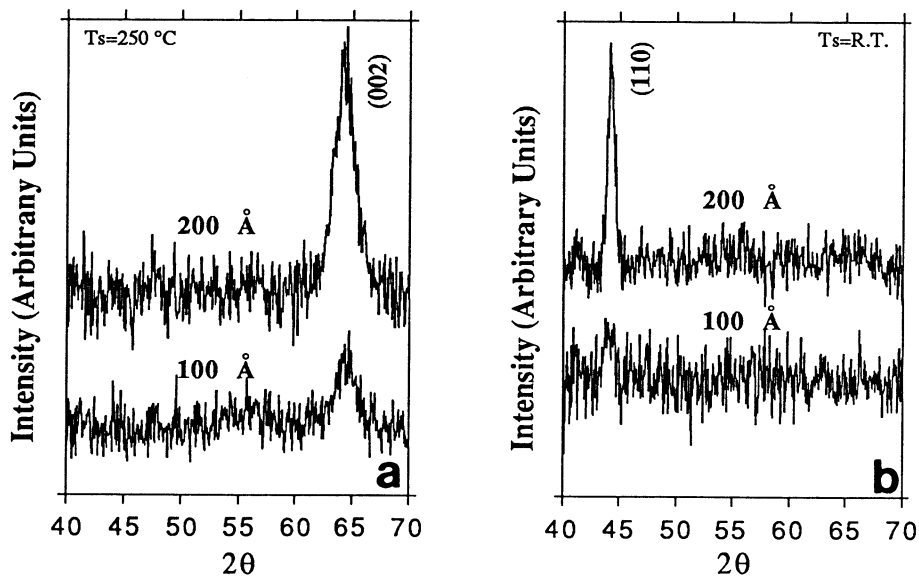


Figure 2. X-ray diffraction patterns of Cr thin films deposited on glass at (a) 250°C, (b) room temperature.

Each of these textures gives rise to a different texture for the subsequently deposited Co-alloy films: the (110) Cr texture gives rise to a  $\{10\bar{1}1\}$  Co-alloy texture and the (002) Cr texture gives rise to a  $\{11\bar{2}0\}$  Co-alloy crystallographic texture. The Co-alloy texture develops from the Cr underlayer by means of epitaxy. We will discuss this mechanism in section II, below. But first we discuss how the different Cr crystallographic textures develop on amorphous substrates.

There are two ways a non-epitaxial texture may develop during the formation of thin films: the texture may form primarily in the nucleation stage of the film or the texture may form primarily during the growth stage of the film.

Figures 2a and 2b display the X-ray diffraction patterns for 10 and 20 nm thick Cr films deposited at room temperature and 250°C respectively. The {002} texture is observed for both the 10 nm and 20 nm film deposited at 250°C, while only the 20 nm film deposited at room temperature has the {110} texture. From this, we see that the {002} crystallographic texture which developed at 250°C is most probably formed during the nucleation stage of the film. However, the {110} crystallographic texture of the Cr films seems to develop during the growth stage for the Cr films deposited under these process conditions. See also reference 18.

If the texture is determined during the nucleation stage, the relative values of three surface energies are important: the substrate/film, the substrate/vacuum and the film/vacuum energies.<sup>19-20</sup> In Figure 3, these values are denoted as S12, S2 and S1 respectively. Furthermore, since the film is crystalline, there are different values of S1, which depend on the crystallographic plane in question. For crystals with the bcc structure, the {110} planes have the lowest surface energy since they are the closest packed ones. The {100} planes have the next lowest surface energy for bcc structures. Looking at Figure 3 it can be seen that a simple force balance applied to these surface energies shows that if the value of S12 is small, the film will wet the surface, and form in the shape shown in Figure 3A. This would give rise to the {110} texture for the growing film, since as indicated above the {110} planes have the lowest surface energies in the bcc structure. On the other hand, if the value of S12 is large, the film will tend to be more equiaxed in shape. To minimize the surface energy of the film the (002) planes would be parallel to the substrate surface since this configuration maximizes the amount of {110} surface area for the developing Cr island. This argument assumes that there is enough time (or energy) available for the film to obtain equilibrium or near equilibrium shapes. This appears to be the case for Cr films when the substrate is pre-heated. Thus the formation of the (002) crystallographic texture can be explained as a nucleation texture.

If there is not enough time for the equilibrium shape to form, the initial orientation of the Cr grains should be nearly random. Any texture that develops in this case would do so during the growth stage of the film. Figure 4 is a schematic showing the growth of two films with differing initial grain sizes. As the films grow, the balance of surface energies would predict that the grains with the {110} surfaces would expand on growth. This can be seen again to be the result of a simple force balance, since any other grain orientation would have a surface with a higher energy parallel to the plane of the film. As shown in the Figure this would tend to expand the (110) oriented grain, hence lowering the overall surface energy. Note also that the film with the smaller grain size would obtain a strong {110} texture at smaller thicknesses than the one with the larger grain size.

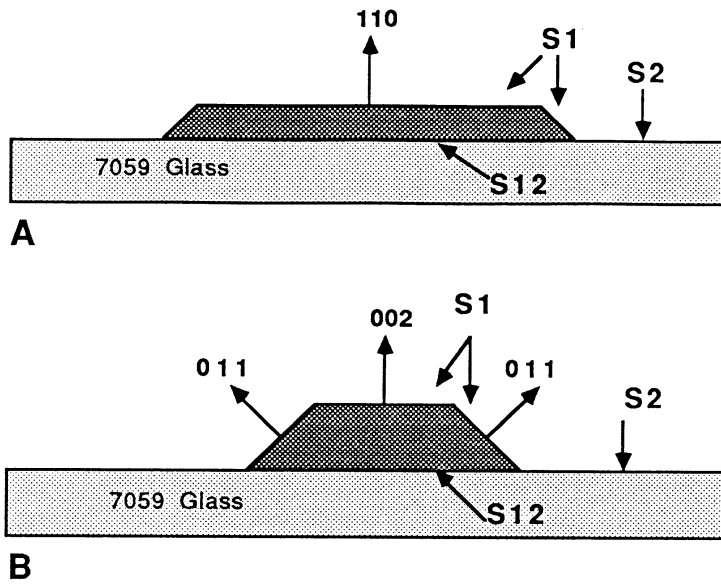


Figure 3. Schematic view of the nucleation of islands of Cr on glass substrates for (a) small values of  $S_{12}$ , (b) large values of  $S_{12}$ . Note that in (b) the shape of the nucleus that minimizes the energy produces the (002) crystallographic texture.

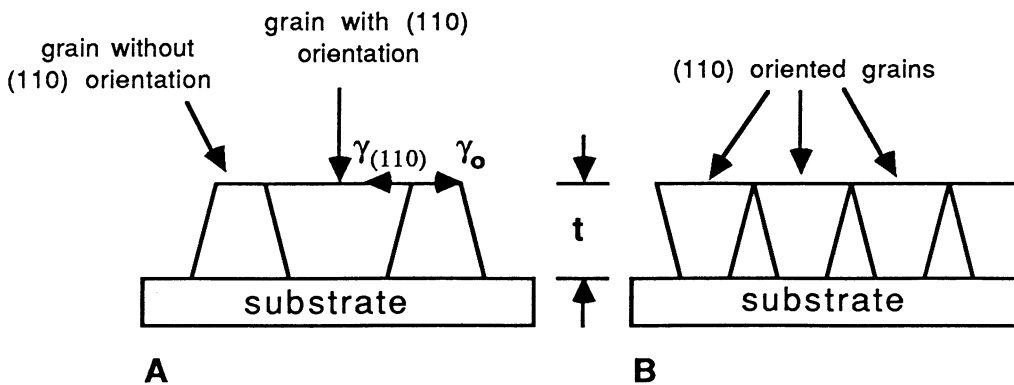


Figure 4. Schematic view of the development of texture during growth of film for (a) large initial grain size, (b) small initial grain size.

As a general rule, the textures which develop during the growth of thin films are those with the closest packed planes parallel to the plane of the film. The growth textures of several structures are listed in Table I.

**TABLE I**  
**Growth Textures**

bcc	$\text{Im}\bar{3}\text{m}$	{110}
fcc	$\text{Fm}\bar{3}\text{m}$	{111}
hcp	$\text{P}\frac{6_3}{\text{m}}\text{mc}$	(0001)
B2	$\text{Pm}\bar{3}\text{m}$	{110}
D03	$\text{Fm}\bar{3}\text{m}$	{110}

This approach to understanding the crystallographic textures of thin films grown on amorphous substrate has been discussed by Feng *et al.*<sup>21</sup>

## II. DEVELOPMENT OF MAGNETIC LAYER CRYSTALLOGRAPHIC TEXTURE

The development of the crystallographic texture of the Co alloy films depends for the most part on epitaxial relationships between the Co alloy film and the underlayer. If no underlayer is used, the Co alloy films (which usually have the hcp structure) are grown on an amorphous substrate, such as glass or amorphous NiP films. The crystallographic texture that develops will be (0001). This is fine if the films are to be utilized in the perpendicular recording mode, but is of little use for longitudinal recording. The use of underlayers has been demonstrated to cause the c axes of the grains of the film to lie in or near the plane of the film.

As mentioned above, two crystallographic textures are well documented for Co alloy magnetic thin films. For Co alloys deposited on (110) Cr textured underlayers, the (10 $\bar{1}$ 1) Co texture is obtained. Figure 5 shows that there is a good match between the atoms on these two planes. Figure 6 shows that the fit between atoms on the (10 $\bar{1}$ 0) planes of Co and some of the atoms on the (110) planes of Cr is also good, but the density of atoms on the planes is very different. The extra atom in the Cr plane would raise the interfacial energy between these planes due to the lack of any atomic bonds across the interface for the extra atom. This orientation relationship in crystallographic texture is not usually reported.

The second well documented texture for the Co/Cr thin films is the (1 $\bar{1}$ 20) Co parallel to the (002) Cr. As indicated above, the (002) Cr crystallographic texture is formed when the substrate is held at elevated temperatures. Figure 7 shows the atomic matching for the case of the (1 $\bar{1}$ 20) of the Co alloy parallel to (002) of Cr. Once again, there is a good match in both the size of the projected unit cell and the number of atoms per unit area of both structures.

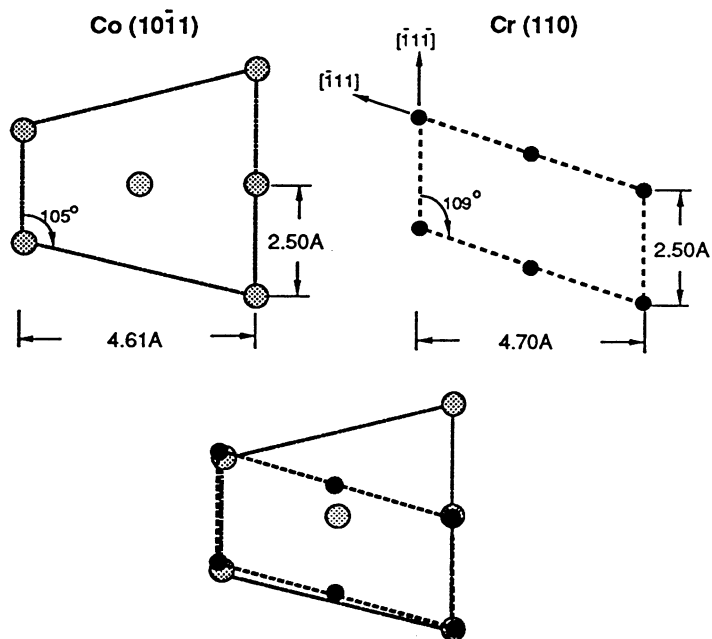


Figure 5 Schematic of the atomic positions of  $(10\bar{1}1)$  Co and  $(110)$  Cr planes.

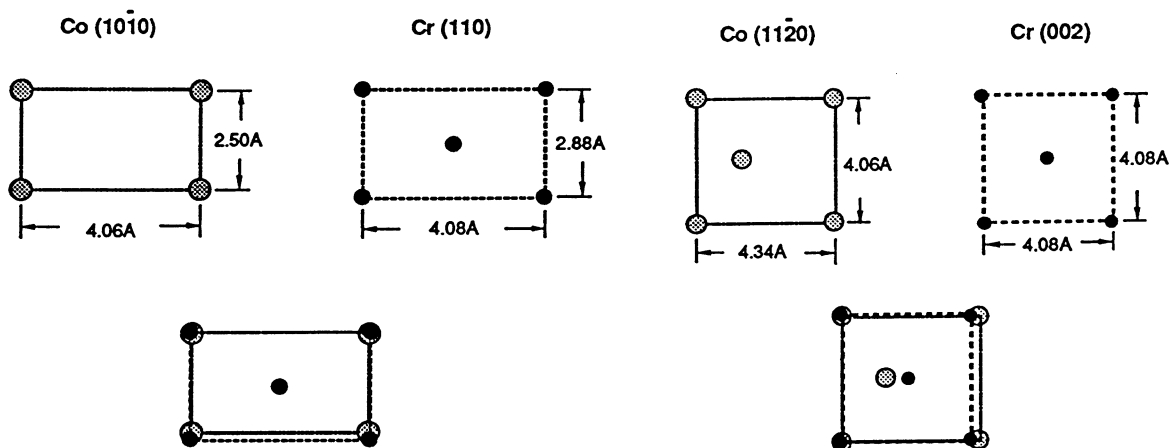


Figure 6 Schematic of the atomic positions of  $(10\bar{1}0)$  Co and  $(110)$  Cr planes.

Figure 7 Schematic of the atomic position of  $(11\bar{2}0)$  and  $(002)$  Cr planes.

In recent work, Lee *et al.*<sup>22</sup> have used NiAl as an underlayer for Co alloy films. The lattice parameter of this material is nearly identical to that of Cr, so it was expected that the same crystallographic texture would result. NiAl (which has the B2, bcc derivative structure) develops a weak (110) texture on deposition. See Table I. However, the Co alloy film develops the (10 $\bar{1}$ 0) crystallographic texture, not the (10 $\bar{1}$ 1) as with a Cr underlayer. See Figure 8. On closer examination of the X-ray pattern, it can be seen that a fairly strong (112) peak also exists for the B2 NiAl films. The atomic matching of (10 $\bar{1}$ 0) Co with (112) of Cr and/or NiAl is shown in Figure 9. It can be seen to be an excellent fit. In fact, other workers<sup>23-24</sup> had reported the (10 $\bar{1}$ 0) texture for Co alloys deposited on Cr, and an inspection of their diffraction pattern showed that their Cr film also had a fairly strong (112) peak. We conclude that this texture: (10 $\bar{1}$ 0) Co alloy parallel to (112) NiAl or Cr is a low energy one. Table II summarizes different orientation relationships that we have observed by means of electron microdiffraction. See references 17, 25 and 26.

---

**TABLE II**  
**Orientation Relationships of Thin Films**

(10 $\bar{1}$ 1) Co	//	(110) Cr
(11 $\bar{2}$ 0) Co	//	(002) Cr
(10 $\bar{1}$ 0) Co	//	(112) Cr
(10 $\bar{1}$ 0) Co	//	(113) Cr

---

Thus the crystallographic textures that develop in Co alloy hcp thin films can all be explained in terms of a best fitting of the atomic planes across the thin film interface. Hence the mechanism of the formation of the initial crystallographic texture of the magnetic layers is that of epitaxy. It should be noted, however, that as the hcp magnetic layers grow thicker, there is a tendency for them to obtain their low energy growth texture, namely the (0001).

Other microstructural features are also affected by this epitaxy, and to these we now turn.

### III. GRAIN SIZE AND CRYSTALLINE PERFECTION

Keeping these various mechanisms of the formation of crystallographic textures in mind, we turn to the application of them to several interesting features. Figure 10 is a schematic drawing which demonstrates the use of an interlayer between two magnetic layers. The identity of this interlayer can vary, though published works to date have used Cr as an interlayer as well as the underlayer. The interlayer serves to "break up" the magnetic layer, and may help to increase the signal to noise ratio of recording due to an effectively smaller "particle size" in the films. The interlayer may form epitaxially on the first magnetic film. If it does, it has a good chance of "passing on" the crystallographic texture of the first magnetic layer to that of the second magnetic layer. Cr interlayers have been shown to do this. See Figure 11.<sup>27</sup> Here the dark field

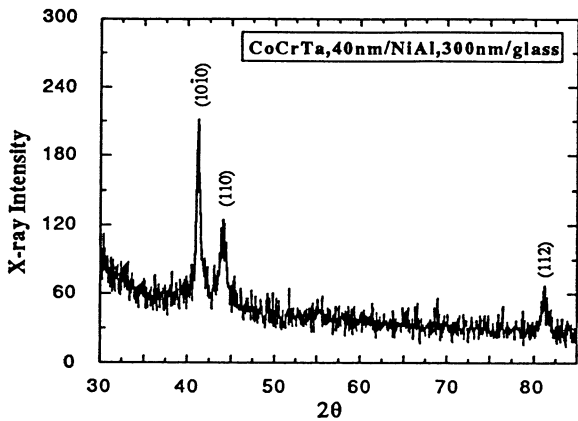


Figure 8  
X-ray diffraction pattern of Co-alloy deposited on 300 nm of NiAl. Note the {112} NiAl peak.

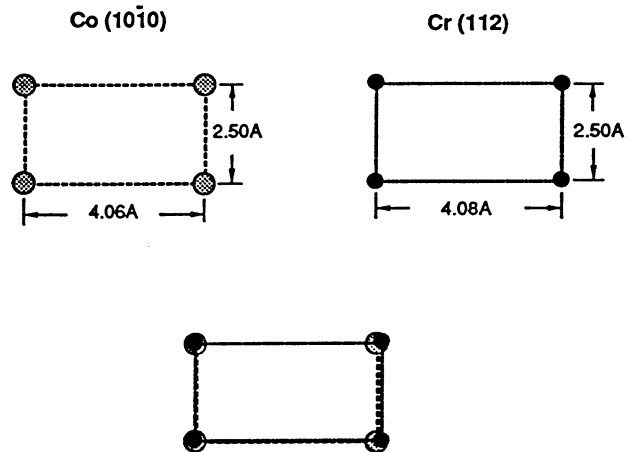


Figure 9  
Schematic of the atomic positions of (1010)Co and (112)Cr (and NiAl) planes.

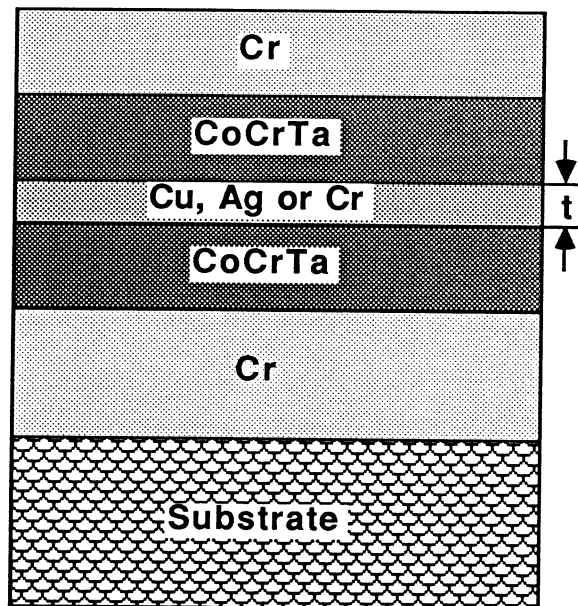


Figure 10. Schematic of thin film configuration including an interlayer.



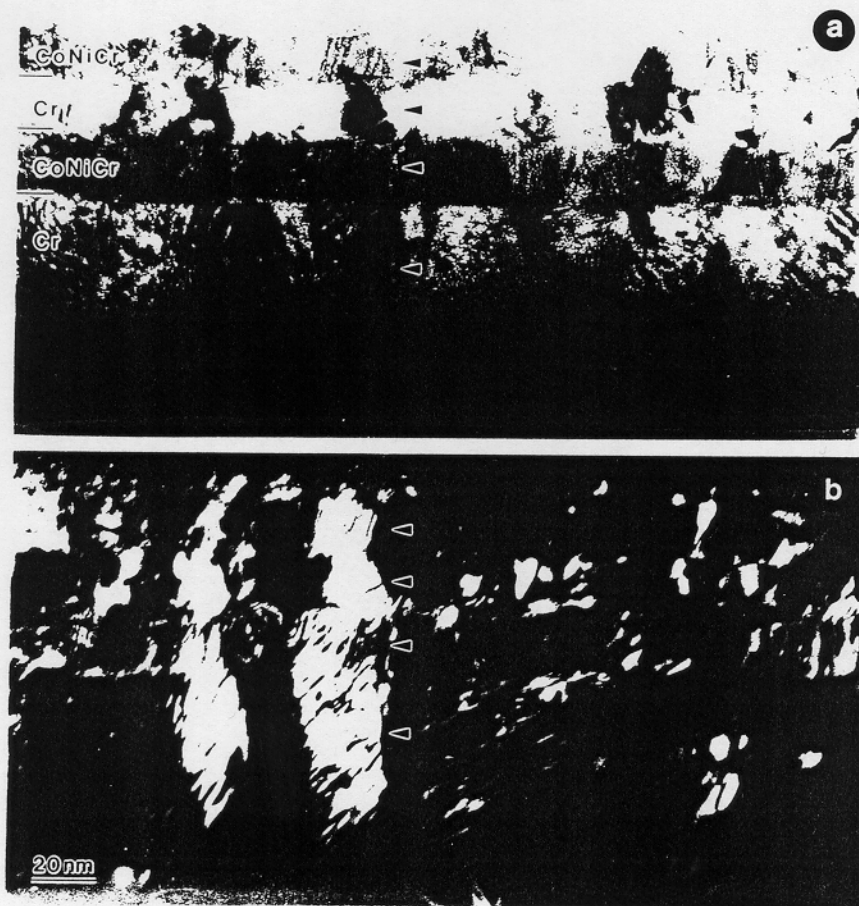


Figure 11. TEM cross section of multilayer film (a) Bright field, (b) Dark field.

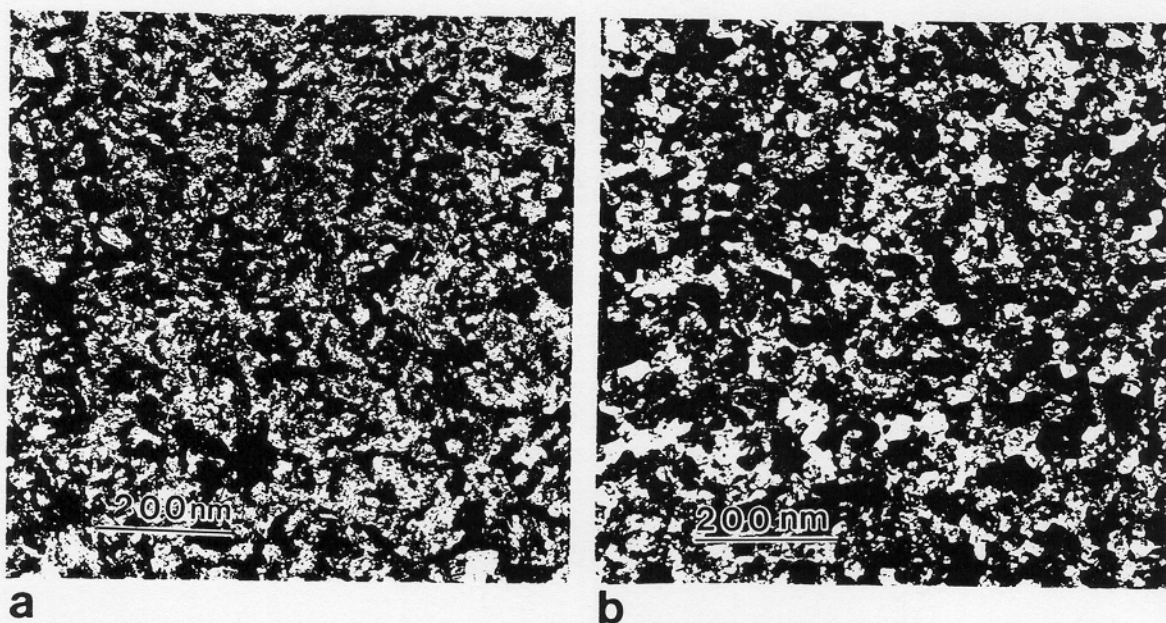


Figure 12. Microstructure of Cr films, 50 nm thick, grown with: (a) no bias, (b) -200 V bias. Notice that the grains in (b) are much more clearly defined.

micrograph clearly shows that several of the columns of the films have bcc and hcp regions that are all correlated to one another. Using other interlayers offers the opportunity of breaking up the crystallographic texture of the magnetic layers, as these metals are fcc in structure. Feng *et al.* have presented preliminary work on this and reported that the results are promising.<sup>28</sup>

Another feature of the use of interlayers is that it helps in the production of magnetic layers with smaller grain size. As reported earlier, the magnetic layer always has a grain size that is the same size or smaller than that of the Cr underlayer. When an interlayer is deposited on the first magnetic layer it will take on the grain size of the magnetic layer. Then, when the second magnetic layer is deposited on the interlayer, it will probably have a grain size that is smaller than that of the interlayer. This mechanism of producing magnetic layer thin films with small grain size is a topic of our current research.

One final interesting topic for discussion is the degree of crystallographic perfection of the underlayers and how that might affect the perfection of and hence the magnetic properties of the subsequently grown magnetic layer. Figures 12a and 12b show TEM microstructures of Cr grains that were deposited with and without applied bias, respectively. The Cr film formed with bias has a much more clearly defined grain structure than the one formed without bias. From high resolution TEM it can be seen that the Cr film formed with an applied bias during sputtering has fewer subgrain boundaries within its grains. This means that it has fewer defects present than the Cr film formed without bias. The magnetic layers which formed on top of these different underlayers will to some extent replicate these features, and thus have differing amounts of defects in them and hence have different magnetic properties. Thus, the control of certain extrinsic magnetic properties of magnetic thin films can be performed by careful control of the conditions by which their respective underlayers are produced.

#### IV. SUMMARY

We have presented a brief overview of various features of the development of crystallographic textures of thin films utilized for magnetic recording. The magnetic thin film obtains its initial crystallographic texture as well as grain size and perfection by means of epitaxy with its underlayer. Various important crystallographic textures between hcp Co alloy films and their metallic underlayers were presented and explained in terms of the atomic arrangement of atoms across the epitaxial interface. The development of the crystallographic texture of the Cr underlayer was discussed. A model for the development of the initial textures during either the nucleation or growth stage of the film was presented. Finally the importance of epitaxy on other microstructural features of the magnetic thin film was discussed.

#### REFERENCES

1. J.P. Lazzari, I. Melnick and D. Randet, *IEEE Trans. Magn.* **3**, 205 (1967).
2. J.P. Lazzari, I. Melnick and D. Randet, *IEEE Trans. Magn.* **5**, 955 (1969).
3. J. Daval and D. Randet, *IEEE Trans. Magn.* **6**, 768 (1970).
4. G.-L. Chen, *IEEE Trans. Magn.* **22**, 334 (1986).
5. R.D. Fisher, J.C. Allen and J.L. Pressesky, *IEEE Trans. Magn.* **22**, 352 (1986).

6. S.L. Duan, J.O. Artman, J.-W. Lee, B. Wong and D.E. Laughlin, *IEEE Trans. Magn.* **25**, 3884 (1989).
7. B.C. Movchan and C.B. Demchishin, *Phys. Met. Metallogr.* **28**, 83 (1963).
8. J.A. Thornton, *J. Vac. Sci. Technol.* **11**, 666 (1974).
9. H.J. Lee, *J. Appl. Phys.* **57**, 4037 (1985).
10. T. Ohno, Y. Shiroishi, S. Hishiyama, H. Suzuki and Y. Matsuda, *IEEE Trans. Magn.* **23**, 2809 (1987).
11. D.P. Ravipati, W.G. Haines, and J.L. Dockendorf, *J. Vac. Sci. Technol.* **A5**, 1968 (1987).
12. D.M. Mattox, *J. Vac. Sci. Technol.*, **A7** (3), 1105 (1989).
13. S.L. Duan, J.O. Artman, B. Wong, and D.E. Laughlin, *J. Appl. Phys.* **67**, 4913 (1990).
14. J. Pressesky, S. Y. Lee, S.L. Duan and D. Williams, *J. Appl. Phys.* **69**, 5163 (1991).
15. T. Yogi, T.A. Nguyen, S.E. Lambert, G.L. Gorman and G. Castillo, *Mat. Sci. Soc. Symp. Proc.* **232**, 3 (1991).
16. J. Lin, C. Wu and J.M. Silvertsen, *IEEE Trans. Magn.* **26**, 39 (1990).
17. K. Hono, B. Wong and D.E. Laughlin, *J. Appl. Phys.* **68**, 4734 (1990).
18. Li Tang and Gareth Thomas, *J. Appl. Phys.* **74**, 5025 (1993).
19. W. L. Winterbottom, *Acta Metallurgica* **15**, 303 (1967).
20. J. W. Cahn and J. Taylor, *Phase Transformations '87*, 545 (1988).
21. Y. C. Feng, D. E. Laughlin and D. N. Lambeth, (unpublished)
22. L.-L. Lee, D.E. Laughlin and D.N. Lambeth (unpublished).
23. Y. Hsu, Q. Chen, K.E. Johnson, J.M. Suvertson and J.H. Judy, *Proceedings of the Second International Symposium on Magnetic Materials, Processes, and Devices of the Electrochemical Society*, **92-10**, 95 (1991).
24. A. Nakamura and M. Futamoto, *Jpn. J. Appl. Phys.* **32**, Pt.2, L1410 (1993).
25. T. Yogi, G. L. Gorman, C. Hwang, M. A. Kakalec and S. E. Lambert, *IEEE Trans. Magn.* **24**, 2727 (1988).
26. David E. Laughlin and Bunsen Y. Wong, *IEEE Trans. Magn.* **27** 4713 (1991).
27. B.Y. Wong and D.E. Laughlin, *J. Appl. Phys. Lett.* **61**, 2533 (1992).
28. Y. C. Feng, D. E. Laughlin and D. N. Lambeth, submitted 6th MMM-INTERMAG.

## ACKNOWLEDGEMENT

Work presented in this review has been sponsored by the Department of Energy (DE-FG02-90ER45423, Y.C.F.), the National Science Foundation (ECD 89-07068, L.L.L.) and Hitachi Metals Limited (B.W.). We thank Prof. David N. Lambeth for many stimulating discussions.